Heritable epigenetic changes are constrained by the dynamics of regulatory architectures

Antony M Jose[1]

ABSTRACT

Interacting molecules create regulatory architectures that can persist despite turnover of molecules. Although epigenetic changes occur within the context of such architectures, there is limited understanding of how they can influence the heritability of changes. Here I develop criteria for the heritability of regulatory architectures and use quantitative simulations of interacting regulators parsed as entities, their sensors and the sensed properties to analyze how architectures influence heritable epigenetic changes. Information contained in regulatory architectures grows rapidly with the number of interacting molecules and its transmission requires positive feedback loops. While these architectures can recover after many epigenetic perturbations, some resulting changes can become permanently heritable. Such stable changes can (1) alter steady-state levels while preserving the architecture, (2) induce different architectures that persist for many generations, or (3) collapse the entire architecture. Architectures that are otherwise unstable can become heritable through periodic interactions with external regulators, which suggests that the evolution of mortal somatic lineages with cells that reproducibly interact with the immortal germ lineage could make a wider variety of regulatory architectures heritable. Differential inhibition of the positive feedback loops that transmit regulatory architectures across generations can explain the gene-specific differences in heritable RNA silencing observed in the nematode *C. elegans*, which range from permanent silencing, to recovery from silencing within a few generations and subsequent resistance to silencing. More broadly, these results provide a foundation for analyzing the inheritance of epigenetic changes within the context of the regulatory architectures implemented using diverse molecules in different living systems.

Keywords: robustness, plasticity, positive feedback, transgenerational epigenetic inheritance, heredity, RNA silencing

Affiliation: [1]University of Maryland, College Park, MD, USA. Email: amjose@umd.edu

INTRODUCTION

Patterns formed by interactions between molecules can be preserved by living systems even as the molecules change over time. For example, the localization and activity of many different kinds of molecules are repeated in successive generations during comparable stages, establishing transgenerational waveforms that preserve form and function [1-3]. At any time, interactions that can be used to predict future arrangements of molecules define regulatory architectures that drive change or preserve homeostasis. Such architectures that arose with the origin of life have diversified since through descent with modification to form the many heritable regulatory architectures that are now transmitted across generations along with the genome.

Interactors that form regulatory architectures can span many scales, but descriptions at particular scales are expected to be most useful for a given experimental technique or approach [4]. For example, molecules can interact to form a complex that both provides output to and receives input from another complex, which in turn might be regulated by an organelle. Such interactions can be described as 'top-down' or 'bottom-up' based on the sequential order in which different levels of organization such as molecules, complexes, organelles, cells, tissues etc. are considered to create an explanatory hierarchy. Considering these multi-scale interaction networks in terms of entities, their sensors, and the sensed properties provides a flexible framework for analysis [3] that can be used to progressively refine models (Fig. S1). In these entity-sensor-property (ESP) systems, all interactors of interest can be conveniently defined as entities with some entities acting as sensors. Such sensors can cause changes in the rest of the system or the environment in response to changes in particular properties of other entities. Some interactors have compositions that change over time (e.g., biomolecular condensates with molecules in equilibrium with other dissolved molecules in the surrounding liquid [5]). Such dynamic interactors can be included by considering them as entities whose integrity and properties depend on the properties of some other entities in the system and/or the environment (see [6] for a similar

definition for degrees of individuality). Defined in this way, all ESP systems capture regulatory architectures that could persist over time even as the interacting entities and sensors change. For example, a gated ion channel acts as a sensor when it responds to an increase in the intracellular concentrations of an ion with a change in conformation, allowing the import of other ions from the extracellular environment. During development, such an ion channel could be replaced by another with similar properties, allowing the persistence of the regulatory relationships. Therefore, the analysis of ESP systems is a useful approach for examining heritable regulatory architectures to inform mechanistic studies that aim to explain phenomena using relationships between specific interactors (e.g., epigenetic inheritance using small RNA, chromatin, 3D genome organization, etc.).

Here I consider the transmission of information in regulatory architectures across generational boundaries to derive principles that are applicable for the analysis of heritable epigenetic changes. Only a small number of possible regulatory architectures formed by a set of interactors are heritable. Their maintenance for many generations requires positive feedback loops. Such heritable regulatory architectures carry a vast amount of information that quickly outstrips the information that can be stored in genomes as the number of interactors increase. Quantitative simulations of perturbations from steady state suggest that these architectures can recover after many epigenetic perturbations, but some resulting changes can become heritable. Transient perturbations reveal diagnostic differences between regulatory architectures and suggest ways to generate heritable epigenetic changes for particular architectures. Unstable architectures can become heritable through periodic interactions with external sources of regulation (e.g., somatic cells for architectures within the germline), revealing a strategy for making a wider variety of regulatory architectures heritable. Transgenerational inhibition that tunes the activity of positive feedback loops in regulatory architectures can explain the gene-specific dynamics of heritable RNA silencing observed in the nematode *C. elegans*.

RESULTS

Information in heritable regulatory architectures grows rapidly with the number of interactors

As cells divide, they need to transmit all the regulatory information that maintains homeostasis. This imperative is preserved across generations through a continuum of cell divisions for all organisms as evidenced by the similarity of form and function in successive generations. Such transmission of regulatory information across generations occurs in conjunction with the sequence information transmitted by replicating the genome during each cell division. The maximal information that can be transmitted using the genome sequence is proportional to its length ($\log_2[4].l = 2l$ bits for l base pairs). To determine how the maximal information transmitted by interacting molecules increases with their number (Table 1), the regulatory architectures that can be formed by 1 to 4 entities were considered. Perpetual inheritance of such regulatory architectures requires sustained production of all the interacting molecules, i.e., every interactor must have regulatory input that *promotes* its production to overcome dilution at every cell division and other turnover mechanisms, if any. Indeed, this requirement was fundamental for conceiving the origin of life [7-10] and remains necessary for its persistence. Therefore, the minimal heritable regulatory architecture (HRA) is that formed by two molecules that mutually promote each other's production (Fig. 1, 'A'), resulting in a positive feedback loop. However, not all positive feedback loops form HRAs. For example, positive feedback loops that promote the transient amplification of changes such as that formed by two molecules that mutually repress each other's production [11] are not compatible with perpetual inheritance because both molecules will be eventually lost by dilution or turnover.

Distinct architectures that can be formed by a set of interacting regulators can be represented as directed graphs that are non-isomorphic and weakly connected [12]. Imposing the need for positive regulation for heritability reveals that only 7 of the 13 possible 3-node graphs formed by 3 interactors can be HRAs and only 125 of the 199 possible 4-node graphs can be HRAs (see Methods for computation). Including either positive or negative regulation for each interaction in a HRA and then selecting only architectures that include positive

regulatory input for every interactor resulted in non-isomorphic weakly connected directed graphs that represent the distinct regulatory architectures that are heritable (Table 1): two entities form one HRA, three form 25, and four form 5604. Thus, with four interactors, the maximal information that can be transmitted using HRAs ($\log_2[5604] \approx 12.45$ bits) surpasses that transmitted by a four base-pair long genome ($\log_2[4].4 = 8$ bits). The combinatorial growth in the numbers of HRAs with the number of interactors thus provides vastly more capacity for storing information in larger HRAs compared to that afforded by the proportional growth in longer genomes.

Genetic and epigenetic perturbations can generate different heritable changes

To examine how each of the 26 simplest HRAs (Fig. 1 and Fig. S2) responds to a perturbation from steady state, ordinary differential equations that describe the rates of change of each entity in each HRA were developed (see Supplementary Information) and used to simulate steady states (Fig. 2 and Fig. S3 to S9). At steady state, the concentrations of all interactors (x_0, y_0, z_0) remain constant because the combination of all regulatory input, which must cumulatively promote the production of each entity $(k_{xy}, k_{yz}, k_{zy}, \text{etc})$, is equal to the turnover of that entity (T_x, T_y, T_z). In principle, a genetic or non-genetic (i.e., epigenetic) perturbation could alter one or more of the following: the concentration of an entity, the strength of a regulatory link, the rate of turnover of each entity, and the polarity of an interaction. Of these, the most widely used perturbation that is easy to accomplish using current experimental techniques is reducing the concentration of an entity/sensor (e.g., using a loss-of-function mutation, knockdown of an mRNA, degradation of a protein, etc.). Indeed, the use of genome editing [13] for removal and RNA interference (RNAi) [14] for reduction of an entity/sensor are common during the experimental analysis of living systems. Therefore, the impact of permanent or transient loss of an entity was examined in detail.

To simulate genetic change, the response after removal of each entity/sensor was examined in turn for each HRA (Table S1, left panels in Fig. 2, Fig. S3 – S9). Deviations from unregulated turnover of the remaining entities (dotted lines, left panels in Fig. 2, Fig. S3 – S9) reveal the residual regulation and are diagnostic of different regulatory architectures. When the removed interactor was an entity with no regulatory input into the other sensors, the remaining two sensors were unaffected (e.g., left panel, loss of *z* in Fig. S3B, S3D, and S3E). Residual promotion resulted in slower decay (e.g., left panels, *y* in Fig. 2C, 2E, and 2H) and residual inhibition resulted in more rapid decay (e.g., left panels, *x* in Fig. 2G; *y* in Fig. 2F, *z* in Fig. 2C, 2D, 2E, and 2H). In some cases, when the remaining architecture was composed of two sensors that promote each other's production, there was continuous growth of both because their new rates of production exceed their rates of turnover (e.g., left panels, *z* in Fig. 2B, S4B, S5B, S7B, S7C, S8B-D). In other cases, the remaining architecture resulted in slower decay of both because their new rates of production were insufficient to overcome turnover (e.g., left panels, *z* in Fig. S4A, S5A, S6A-D, S8A).

To examine scenarios where epigenetic perturbations could cause heritable changes, the threshold for observing a defect was set at 0.5x of the steady-state levels (dotted line, right panels in Fig. 2, Fig. S3 – S9). RNAi can cause detectable defects that are heritable [14] and the conditions that promote or inhibit heritable epigenetic change after RNAi of a gene have been proposed to depend upon the regulatory architecture [15]. To simulate RNAi of an entity/sensor, the response after a transient reduction of each entity/sensor to 2x below the threshold required for observing a defect was examined in turn for each HRA (right panels in Fig. 2, Fig. S3 – S9). The responses after this transient epigenetic perturbation were different from that after genetic perturbation (compare left and right in Fig. 2 and Fig. S3 – S9), as expected. Many HRAs recovered the levels of all entities/sensors above the threshold required for detecting a defect (e.g., right panels in Fig. 2B, 2C, 2D, 2E, and 2H). In some cases, this perturbation was sufficient to maintain the architecture but with a reduced steady-state level of all entities/sensors (e.g., reduction of *x* in Fig. 2A, right; Fig. S3B-E, right; Fig. S4B, right; Fig. S7C, right). Notably, whether recovery occurs with the steady-state levels of each entity/sensor returning above or below the threshold for observing a defect depended not only on the architecture, but also on the identity of the perturbed entity/sensor (e.g., compare reduction of *x* vs. *y* in Fig. S3A, right; *x* vs.

y or *z* in Fig. S2B, right; *x* vs. *y* or *z* in Fig. S3C, right). Transient reduction of other entities/sensors below the threshold for observing defects was also observed in many cases (e.g., levels of *z* when *x* was perturbed in Fig. 2C, right; of *z* when *y* was perturbed in Fig. 2D, right; of *z* when *x* was perturbed in Fig. 2E, right; of *x* and *y* when *z* was perturbed in Fig. 2H, right). In some cases, recovery of original architectures occurred even after complete loss of one entity/sensor (e.g., after transient loss of *z* in Fig. 2G, right; of *y* in Fig. S8B, right; of *y* in Fig. S8D, right). Such recovery from zero can be understood as re-establishment of the regulatory architecture within the duration of simulation (100 in Fig. 2, Fig. S3 – S9) and is analogous to basal activity in the absence of inducers (e.g., leaky production of LacY permease from the *lac* operon in the absence of lactose [16], which allows the initial import of the lactose required for activating the *lac* operon). Alternatively, such recovery can also be understood as arising from the production of the missing entity/sensor as a byproduct when the activity of the upstream regulator increases beyond a threshold. Transient perturbations were also observed to induce different architectures that can persist for many generations (e.g., transient reduction of *z* resulting in loss of *y* and mutually promoted growth of *x* and *z* in Fig. 2F, right; also see Fig. S8E and S9A). Such continuous growth after an epigenetic change provides opportunities for achieving new steady states through dilution via cell divisions during development, potentially as part of a new cell type. Finally, some transient perturbations also led to the collapse of the entire architecture (e.g., transient perturbation of *y* in Fig. S9A, right).

In summary, genetic and epigenetic perturbations from steady state can cause a diversity of changes in HRAs that constrain the possible regulatory architectures consistent with experimental data obtained by perturbing them. HRAs that are nearly indistinguishable by genetic perturbation can be distinguished using epigenetic perturbations, underscoring the complementary nature of genetic and epigenetic perturbations.

Changes in HRAs caused by single mutations form a sparse matrix

Just as mutations in a DNA genome can persist through replication at each cell division, changes in HRAs can persist by the formation of new positive feedback loops or the liberation of previously inhibited positive feedback loops. Six types of changes in sequence can arise from the four bases in a DNA genome upon mutation (A‹–›T, A‹–›G, A‹–›C, T‹–›G, T‹–›C, G‹–›C, with density of the change matrix = 1 [6/6]). To determine the analogous types of changes in regulatory architectures, the capacity for each of the 26 simplest HRAs (A to Z in Fig. 1) to change into other HRAs was considered (Fig. 3). Single perturbations of any interactor (entity/sensor) could result in the loss of the interactor, loss of an interaction, or a change in the polarity of an interaction (e.g., [17]). These perturbations could 'mutate' the HRA by either collapsing the entire architecture or stably changing it into a new HRA (Fig. 3). Only changes that do not eliminate all positive regulatory inputs to an interactor can result in the persistence of a regulatory architecture rather than the eventual loss of one or more entities. Furthermore, since at steady state all gain of an entity/sensor is balanced by loss (via dilution at every cell division and/or other turnover mechanisms), any *permanent* reduction in the promotion of an entity/sensor will ultimately lead to its loss. Finally, if there is promotion of one sensor in a positive feedback loop and inhibition of another sensor in the same positive feedback loop, then the net input can be positive or negative depending on the relative magnitudes of the inputs. With these considerations, enumeration of the changed HRAs that can result from a perturbation revealed that the 26 HRAs can be mutated to generate 61 different changes (24 through loss of interaction alone, 21 through change in polarity of interaction alone, and 16 through either change in regulation or though loss of an entity, with density of the change matrix ≈ 0.19 [61/325]). Thus, unlike changes in DNA sequence, not all changes are immediately accessible among HRAs (change matrix of 1 vs. 0.19, respectively). Nevertheless, the heritable information transmitted using regulatory architectures is vast because even two or three interactors can form 26 heritable architectures that are collectively capable of 61 changes through single perturbations. This capacity is an underestimate because, single mutations can also result in the gain of new interactions that combine multiple HRAs into larger regulatory architectures with more interactors.

The constrained transition from one HRA at steady state to the next adjacent HRA through a single change (Fig. 3) could skew the frequencies of different HRAs observed in nature and restrict the mechanisms available for development and/or evolution. For example, the HRA 'A' is accessible from 16 other HRAs but 'C' and 'T' are each accessible only from one other HRA ('J' and 'U', respectively). Furthermore, HRAs that rely on all components for their production ('C', 'F', 'H', 'K', and 'T') cannot change into any other HRAs from steady state without the addition of more positive regulation because any permanent loss in regulation without compensatory changes in turnover will result in the ultimate collapse of the entire architecture. These constraints can be overcome if change can occur through regulatory architectures that are not indefinitely heritable.

Deducing regulatory architectures from outcomes after perturbations is complicated by multiple HRAs resulting in the same HRA when perturbed (e.g., 16 HRAs can result in 'A' when perturbed, Fig. 3). While measurement of dynamics after perturbations of *each* entity/sensor in turn can distinguish between all 26 architectures, the temporal resolution required is not obvious. This difficulty in accurate inference is apparent even for the simplest of perturbation experiments when inference relies only on end-point measurements, which are the most common in experimental biology. For example, a common experimental result is the loss of one regulator (*x*, say) leading to an increase in another (*y*, say), which is frequently interpreted to mean *x* inhibits *y*. However, an alternative interpretation can be that *y* promotes *x* and itself via *z*, which competes with *x*. In this scenario, removal of *x* leads to relatively more promotion of *z*, which leads to a relative increase in *y*. These equivalent outcomes upon loss or reduction of an entity in different architectures highlight the difficulty of inferring the underlying regulation after perturbation of processes with feedback loops. Therefore, simulations that enable exploration of outcomes when different interactors are perturbed at different times could enhance the understanding of underlying complexity, reduce biased inference, and better guide the next experiment.

Simple Entity-Sensor-Property systems enable exploration of regulatory architectures

The most commonly considered regulatory networks [18] are either limited in scope and/or are not causal in nature. For example, gene regulatory networks [19] consider transcription factors, promoter elements, and the proteins made as the key entities. Additional specialized networks include protein-protein interaction networks (e.g., [20]), genetic interaction networks (e.g., [21]), and signaling networks (e.g., [22]). However, regulation of any process can rely on changes in a variety of molecules within cells, ranging from small molecules such as steroid hormones to organelles such as mitochondria. Furthermore, experimental studies often seek to provide explanations of phenomena in terms of a diversity of interacting entities. A common expression for all possible regulatory networks that preserves both causation and heritability can be derived by parsing all the contents of the bottleneck stage between two generations (e.g., one-cell zygote in the nematode *C. elegans*) into entities, their sensors, and the sensed properties [3]. An additional advantage of such entity-sensor-property systems is that it is possible to consider entities that are sensed by a particular sensor even via unknown intermediate steps, allowing for simulation of regulatory networks despite incomplete knowledge of regulators.

For a given genome sequence, the number of distinguishable configurations of regulators represented as entities and sensors is given by the following equation [3]:

$$c_{tot} = \sum_{i=1}^{b} e_i \left(\sum_{j=1}^{s_i} s_j \left(\sum_{k=1}^{p_j} p_k \right) \right) \qquad (1)$$

where, e is the measured entity (total b in the bottleneck stage between generations: n_b in system, o_b in environment), s is the measuring sensor (total s_i for i^{th} entity), which is itself a configuration of entities drawn from the total N per life cycle (i.e., $f(Y)$, with each $Y \subseteq \{e_1, e_2, \ldots, e_N\}$), and p is the attainable and measurable values of the property measured by the sensor (total p_j for the jth sensor of the ith entity). An entity or configuration of entities is considered a sensor only if changes in its values can change the values of other entities in the system or in the environment at some later time.

The complex summation $\sum_i e_i \sum_j s_j \sum_k p_k$ can be simplified into a product of measurable

property values of individual entities/sensors if the possible numbers of property values of every entity/sensor combination is independent:

$$c_{tot} = \prod_{i=1}^{b} \prod_{j=1}^{s_i} n_{ij} \qquad (2)$$

where, $n_{ij} = |\{p_1, p_2, \dots p_j\}|$ is the number of property values as measured by the jth sensor of the ith entity. However, this upper limit is never reached in any system because regulatory interactions make multiple sensors/entities covary [3]. As a simple example, consider two sensors that activate each other in a Boolean network with no delay: the only possible values are {0,0} when both sensors are off and {1,1} when both sensors are on, because the mutual positive regulation precludes {0,1} and {1,0}.

Three simplifying assumptions were made to facilitate the simulation of regulatory networks with different architectures: (1) let the number of molecules be the only property measured by all sensors, (2) let each sensor be a single kind of molecule, and (3) let all entities be within the system. In these simple Entity-Sensor-Property (ESP) systems, the number of possible configurations is given by:

$$c_{tot} = \sum_{i=1}^{E} e_i \left(\sum_{j=1}^{s_i} n_j \right) < \prod_{i=1}^{E} \prod_{j=1}^{s_i} n_{ij} \qquad (3)$$

where, e is the measured entity (total E in the system), s is the measuring sensor (total s_i for i^{th} entity), n_j is the attainable and measurable numbers of the ith entity, and n_{ij} is the attainable and measurable numbers of the ith entity as measured by the jth sensor. In such simplified ESP systems, a sensor is simply an entity in the system that responds to changes in numbers of an entity by changing the numbers of that entity or another entity. Whether downstream changes occur depends on the sensitivity of the sensor and the step-size of changes in property value (i.e., number) of the downstream entity/sensor.

A hybrid approach with deterministic and stochastic aspects was used to simulate ESP systems (e.g., Fig. 4A) represented by equation (3) with random values for the numbers of each entity/sensor, the sensitivity of each sensor (i.e., the change in number needed to change a downstream entity/sensor), the step-size of changes in property (i.e., numbers changed per input from a sensor), and the active fraction (i.e., proportion that are available for interactions at any time). Only an arbitrary fraction of each entity (fixed over time) was simulated as active to account for processes such as folding, localization, diffusion, etc., that can limit regulatory interactions. Simulations were begun with a total of 500 molecules. A maximal increase of 5,000 molecules was allowed per cell cycle before each cell division to account for depletion of precursors, reactants, or building blocks (which were not explicitly simulated). The simulation was ended if total number of simulated molecules increased beyond a maximal number (500,000 in Fig. 4) to account for the limited capacity of a cell. Thus, with each time step, the numbers of all entities/sensors changed deterministically based upon the randomly established initial regulatory architecture with stochastic changes in the numbers of each entity arising from the random order of evaluation at each time step and the reduction by ~1/2 at the start of each cell cycle, which simulates experimentally observed noise (e.g., [23]). With these parameters, regulatory architectures were simulated and the relative concentration of each entity/sensor was plotted over time (Fig. 4A). These profiles represent the change in 'phenotype' over time and are akin to measurements of relative RNA abundance using RNA-seq [24] or relative protein abundance using proteomic approaches [25]. Thus, ESP systems represent networks or graphs with weighted edges (because of the different activities of different sensors needed for the transmission of each regulatory change), complex nodes (because of the multiple properties of each entity/sensor), and transmission delays (because of the variation in the duration of each regulatory interaction). Notably, the relative concentrations of an entity can change over time (e.g., 'c' in Fig. 4A) while the underlying regulatory architecture is preserved (see Fig. S10, Movie S1, section titled 'Exploration of Simple ESP Systems' in Supplementary Information, and run 'ESP_systems_single_system_explorer_v1.nlogo' in NetLogo [26] for exploration).

ESP systems differ in their susceptibility to heritable epigenetic changes

Explorations of ESP systems revealed that some systems can be stable for a large number of cell divisions (or equivalently generations) before the level of an entity/sensor becomes zero (e.g.,

system-id 62795 was stable for 59,882.5 generations (Fig. S11)). This long, yet finite duration of stability highlights the difficulty in claiming any architecture is heritable forever if one of its entities/sensors has low abundance and can be lost with a small probability. Systems responded to transient perturbations that reduce the levels of a randomly chosen entity/sensor in two major ways: Type I systems recovered relative levels of entities/sensors, and maintained the same regulatory architecture; Type II systems changed by losing one or more entities, resulting in new relative levels of entities/sensors, and new regulatory architectures that persisted for many subsequent generations. These two types were observed even when the numbers of some entities/sensors were changed by just 2-fold for a few generations (Fig. 4B versus Fig. 4C).

For systematic analysis, architectures that could persist for ~50 generations without even a transient loss of any entity/sensor were considered HRAs and perturbations (loss-of-function, gain-of-function, or none) were delivered at five different times with respect to the start of the simulation (i.e., phases). For loss-of-function, the numbers of one randomly selected entity/sensor was held at half the minimal number of all entities/sensors for 2.5 generations every 50 generations. This perturbation is like the loss of transcripts through RNA interference. For gain-of-function, the numbers of one randomly selected entity/sensor was held at twice the maximal number of all entities/sensors for 2.5 generations every 50 generations. This perturbation is like overexpression of a particular mRNA or protein. Of 225,000 ESP systems thus simulated, 78,285 had heritable regulatory architectures that remained after 250 generations (system-ids and other details for exploration of individual systems are in Table S2). These persistent systems included entities/sensors with relative numbers that changed over time as well as those with nearly constant relative numbers. For each number of interactors considered (2 to 16), only a fraction of the regulatory architectures were stable, plateauing at ~50% of simulated systems with 10 or more entities/sensors (Fig. S12, *top left*). This plateau is likely owing to the limit set for the maximal number of molecules in the system because most systems with many positive regulatory links quickly reached this limit. Although systems began with up to 16 entities/sensors, by the end of 250 generations, there was a maximum of ~8 entities/sensors and a median of ~4 entities/sensors in stable systems (Fig. S12, *bottom left*). Furthermore, an excess of positive regulatory links were needed to sustain a system with negative regulatory links (Fig. S12, *right*), with the minimal system that can sustain a negative regulatory interaction requiring three sensors, as expected. This bias reflects the inability of negative regulatory interactions alone to maintain regulatory architectures over time across cell divisions.

Periodic rescue or perturbation can expand the variety of heritable regulatory architectures

Since the relative abundance of each entity/sensor is expected to trace a transgenerational waveform [2] and to fluctuate with each time step, the relative timing of the perturbations (i.e., their phase) can impact the persistence of particular regulatory architectures. Specifically, entities/sensors with low numbers could be rescued from reaching zero by well-timed gain-of-function perturbations and those with high numbers could be rescued from arresting the simulation by well-timed loss-of-function perturbations. Therefore, the fractions of persistent ESP systems that showed heritable epigenetic change through loss of one or more entities were examined by starting with 2 to 16 molecules for each phase and type of perturbation (Fig. 4D). As expected, only HRAs with a minimum of 3 entities/sensors at the start of the simulation showed heritable epigenetic changes. Fractions of HRAs showing heritable epigenetic changes were comparable across all perturbations for a given number of starting entities/sensors, with more such HRAs identified with increasing numbers of starting entities/sensors (compare Fig. 4D, *top*, *middle*, and *bottom*). The variations in the numbers identified for different phases of perturbation when starting with a particular number of entities/sensors was comparable to the variation observed in systems that were not perturbed (compare Fig. 4D, *top* with Fig. 4D, *middle* and *bottom*), suggesting that no particular phase is more effective. Although some architectures were unaffected by all perturbations, many showed an altered response based on both the nature and phase of the perturbations. Consider the behavior of the illustrative example defined by system-id 46357 that begins with 5 entities/sensors (see Movie S2 to Movie S12). The unperturbed ESP system stabilizes

with an architecture of 3 entities (of the type 'E' in Fig. 1) until ~74 generations, when one of the entities is lost and the new architecture (of the type 'A' in Fig. 1) remains stable until ~286.5 generations. However, perturbations yield a variety of different stabilities depending on phase and type of perturbation. Periodic loss-of-function perturbations with phase '0', '3', or '4' resulted in stability of all 3 entities until collapse at ~130.5, ~181.5, or ~99.5 generations, respectively. But, such perturbations with phase '1' resulted in an earlier change from type 'E' to type 'A' with collapse at ~193.5 generations and with phase '2' resulted in a later change from 'E' to 'A' with collapse at ~184.5 generations. On the other hand, periodic gain-of-function perturbations with phase '0', '1', '2', or '4' prolonged the type 'E' architecture until ~306, ~253, ~212, or ~708 generations, respectively, after which the new type 'A' architecture persisted beyond 1000 generations, by when the simulation was ended. However, such perturbations with phase '3' preserved the type 'E' architecture until collapse at ~311.5 generations.

Collectively, these results reveal that the heritability of regulatory architectures that are intrinsically unstable can be enhanced through interactions that alter the regulation of one or more sensors. Such external regulators could be part of the environment (e.g., periodic interactions such as circadian signals) or other cells (e.g., periodic interactions with somatic cells for regulatory architectures transmitted along a germline).

Organismal development can permit HRAs that incorporate interactions with somatic cells and intergenerational delays in regulation

While for unicellular organisms, each cell division results in a new generation, for multicellular organisms, transmission of heritable information across generations occurs along a lineage of cells that can include many cell divisions with periods of quiescence and interactions with somatic cells. The nematode *C. elegans* is a well-characterized multicellular organism [27] that has many features such as the early separation of the germline during development, sexual reproduction, and the generation of different somatic tissues (Fig. 5A, *top*), that can be incorporated into simulations and are useful for generalization to other animals, including humans. For example, 14 cell divisions are necessary to go from the zygote of one generation to the zygote of the next (Table S3). The loading of oocytes with maternal molecules in multiple organisms makes one generation of delay in regulation (i.e., maternal regulation) common, but such ancestral effects could last longer in principle (e.g., grandparental effects are easily imagined in humans because oocytes begin developing within the female fetus of a pregnant woman). Indeed, studies on RNA silencing in *C. elegans* have revealed long delays in regulation within the germline. For example, parental *rde-4* can enable RNA silencing in adult *rde-4(-)* progeny [28]. Furthermore, loss of *meg-3/-4* can result in persistent RNA silencing defects despite restoration of wild-type *meg-3/-4* for multiple generations [29-31]. However, examining the impact of such long delays and of interactions with somatic cells (e.g., [32]) is computationally expensive. Therefore, to simulate regulatory architectures that persist from one zygote to the next while satisfying some of the known constraints of *C. elegans* lineage and development, the ESP simulator was modified to incorporate the observed timings of cell division versus growth along the germline (Table S3, based on [33-38]) and allow a delay of up to 2 generations for the impact of a regulatory interaction (Fig. 5B).

Since many genes expressed in the germline can be required for fertility or viability, the analysis of how they are regulated across generations poses a challenge. Following the behavior of a reporter across generations provides a proxy that can be used to understand transgenerational regulation in a relatively wild-type background (i.e., the tracer approach [1]). However, regulatory interactions that rely on the gene product will not be re-created by the reporter. For example, the mRNA sequence used to produce antisense small RNA of the gene will differ from that used for the reporter.

To simulate the regulation of a germline gene and its reporter, a modified ESP system is required. In addition to a minimal positive feedback loop required for heritability, positive and negative regulators that depend on *cis*-regulatory sequences shared by both the gene and its reporter as well as such regulators that depend on the different products (e.g., the mRNA and/or protein of gene versus reporter) need to be simulated. Of the 10,000 such ESP systems simulated, 11 maintained all entities/sensors for 10 generations (Table S4). A representative such system (Fig. 5C) forms a HRA

that incorporates regulatory delays ranging from 0 to 171 hours and can persist for hundreds of generations. Examining the levels of all entities/sensors over the first 10 generations (Fig. 5D) reveals that despite starting at random values the HRA settles with a reproducible pattern during each generation (gen 2 onwards in Fig. 5D). The transgenerational waveforms traced by the relative numbers of all entities/sensors reveal periods of increased expression/activity for some entities/sensors during development (red asterisks in Fig. 5D), as observed for many genes expressed in the germline. Future studies that obtain data on key regulators with spatial and temporal resolution can be used to discriminate between different HRAs that drive the expression of different genes of interest.

Differences in negative feedback acting across generations can explain the different durations of heritable RNA silencing in *C. elegans*

The simple fact that organisms resemble their parents in most respects provides evidence for the homeostatic preservation of form and function across generations. Yet, this 'transgenerational homeostasis' [1] is overcome in some cases such that epigenetic changes persist for many generations (reviewed in [39]). Indeed, DNA methylation patterns of unknown origin are thought to have persisted for millions of years in the fungus *C. neoformans* [40]. Studies on RNA silencing in *C. elegans* (reviewed in [41]) provide strong evidence for heritable epigenetic changes in the expression of particular genes, facilitating analysis. When a gene expressed in the germline is silenced using double-stranded RNA of matching sequence and/or germline small RNAs called piRNAs, the silencing can last from one or two generations to hundreds of generations [42-44]. The maintenance of RNA silencing across generations is thought to require a positive feedback loop formed by antisense small RNAs called 22G RNAs that are bound to the Argonaute HRDE-1 [45] and sense mRNA fragments processed into poly-UG RNAs (pUG RNAs) [46] that can act as templates for RNA-dependent RNA polymerases that synthesize the 22G RNAs. However, this mechanism does not explain the variety of effects that can arise when such genes with long-term silencing are exposed to other genes of matching sequence [42, 47]. For example, when a gene silenced by disrupting RNA regulation within the germline (*iT*, a transgene with silenced *mCherry* sequences) is exposed to genes with matching sequences (Fig. 6A, [42]), different outcomes are possible. After initial silencing *in trans*, the newly exposed genes can recover from silencing (*mCherry* and *mCherry*Δ*pi* in Fig. 6A) when separated from the source of silencing signals, but can be either continually silenced (*mCherry/iT* in Fig. 6A) or become resistant to silencing (*mCherry*Δ*pi/iT* in Fig. 6A) depending on the presence of intact piRNA-binding sequences despite the continued presence of the source. While this observation suggests that recognition of the target mRNA by piRNAs prolongs RNA silencing, loss of the Argonaute PRG-1 that binds piRNAs and regulates more than 3000 genes in the germline (e.g., [48]) also prolongs the duration of heritable RNA silencing [43]. Recent consideration of competition for resources in a populations of genes that are being silenced led to a theory based on Little's law of queueing that can explain some observations on RNA silencing in *C. elegans* [49]. Specifically, assuming a pool of M silenced genes with an average duration of silencing of T, new silenced genes arise at a rate λ given by M = λT. However, this theory cannot predict which gene is silenced at any given time, why some genes are initially susceptible to silencing but subsequently become resistant (e.g., *mCherry*Δ*pi* in Fig. 6A), and why the silencing of some genes can last for hundreds of generations. Thus, there is a need for understanding the origins of gene-specific differences in the dynamics of heritable epigenetic changes.

22G RNAs and pUG RNAs are experimentally measurable molecular markers whose levels are thought to be proportional to the extent of gene silencing (e.g., [50-52]), although formally gene-specific regulatory features could influence this proportionality [53]. To understand how the activity of the underlying positive feedback loop that maintains the levels of these RNAs could relate to the extent of observed silencing, the HRDE-1-dependent loop was abstracted into a minimal positive feedback loop with 22G RNAs and pUG RNAs promoting each other's production (Fig. 6B, *top*). Ordinary differential equations (Fig. 6B, *bottom*) were developed for interdependent change in both RNAs by considering their rates of promotion (k_{xy} for 22G and k_{yx} for pUG) and

turnover (T_x for 22G and T_y for pUG). All molecules and chemical modifications that are necessary to maintain a positive feedback loop are sensors because they need to transmit the change from an 'upstream' regulator to a 'downstream' regulator. This 22G-pUG positive feedback loop thus represents mutual promotion by two sensors (i.e., the HRA 'A' in Fig. 1). When any changed molecule or chemical modification is thus viewed as one component of a heritable regulatory architecture driven by a positive feedback loop, two criteria that impact the duration of epigenetic changes through the reduction of particular sensors are immediately suggested: (1) for every permanent change that is observed, all sensors that participate in the regulatory loop must be reduced to a level below that required for observing the change; and (2) for eventual recovery from a change, at least one sensor should be above the threshold required to drive the increase of all other sensors above their respective levels for observing the change. Consistently, a weak and brief reduction of 22G RNAs from steady state levels results in the eventual recovery of both 22G RNA and pUG RNA levels above the threshold required for them to be effective for silencing (Fig. 6C, *left*). Stronger (Fig. 6C, *middle*) or longer (Fig. 6C, *right*) reductions can result in new steady-state levels for both RNAs that are below the threshold required for silencing.

To obtain an analytic expression for how long heritable RNA silencing needs to be inhibited for eventual recovery, the impact of transient reduction in the activity of the $22G\text{-}pUG$ positive feedback loop from steady state ($[22G]_0$ and $[pUG]_0$) was considered. Let $d_x.[22G]_0$ or lower be insufficient for silencing, and let 22G RNAs be transiently perturbed to $p.d_x.[22G]_0 \neq 0$, where $d_x < 1$ and $p < 1$. The critical duration (t_{22G}) of such a perturbation for permanent reduction of 22G RNA below the level required for silencing is given by

$$t_{22G} > \frac{1}{T_y} ln \left[\frac{\frac{1}{d_x.p} - 1}{\left(\frac{1}{p} - 1\right)\left(\frac{T_y}{T_x} + 1\right)} \right] \quad (4)$$

where T_x and T_y are the rates of turnover for 22G RNAs and pUG RNAs, respectively. Analogously, the critical duration (t_{pUG}) of such a perturbation for permanent reduction of pUG RNA below the level required for silencing is given by

$$t_{pUG} > \frac{1}{T_x} ln \left[\frac{\frac{1}{d_y.p} - 1}{\left(\frac{1}{p} - 1\right)\left(\frac{T_x}{T_y} + 1\right)} \right] \quad (5)$$

where $d_y.[pUG]_0$ or lower is insufficient for silencing. Derivation of the general case for these equations (HRA 'A') is presented in supplementary information. These equations suggest that depending on the parameters of the architecture, different sensors may be more easily perturbed to cause heritable epigenetic changes. For example, for the same critical threshold below steady state ($d_x = d_y = 0.5$) and the same extent of perturbation ($p = 0.8$), an architecture with $[22G]_0 = 10$, $[pUG]_0 = 7.14$, $T_x = 0.05$, $T_y = 0.1$, $k_{xy} = 0.07$, $k_{yx} = 0.0714$, is more quickly inhibited by reducing 22G RNAs than by reducing pUG RNAs (6.93 vs. 27.72 units of time).

Combining these considerations with the observations that both piRNA binding to target mRNAs (Fig. 6A) and loss of the piRNA-binding Argonaute PRG-1 [43, 44] prolong the duration of heritable RNA silencing suggests a unified mechanism that sets gene-specific durations of heritable RNA silencing. Specifically, the dynamics of recovery from silencing depends on the strength of an inhibitory feedback that can act across generations to reduce the HRDE-1-dependent positive feedback loop. This transgenerational inhibition relies on sensor(s) that are regulated by PRG-1 and is opposed by piRNA binding to the silenced mRNA (Fig. 6D).

This proposed mechanism implies the existence of sensor(s) that respond to the activity of the HRDE-1-dependent positive feedback loop by recognizing one or more of the molecules and/or chemical modifications generated. Consistently, a chromodomain protein HERI-1 has been reported to be recruited to genes undergoing heritable RNA silencing and is required to limit the duration of the silencing [54]. Additional sensors are likely among the >3000 genes mis-regulated in animals lacking PRG-1 [43, 48]. The levels or activities of these sensor(s) could either increase or decrease in response to the activity of the HRDE-1-dependent loop depending on which of the multiple equivalent configurations of the negative feedback are present at different genes (expected to decrease in Fig. S13, *left* and *right*, but increase in Fig. S13, *middle*). However, in every case, the net result is a reduction

in the activity of the HRDE-1-dependent loop (Fig. S12). Therefore, genes encoding such sensors could be among the genes that show increased mRNA levels (e.g., 2517 genes in [48]) and/or that show decreased mRNA levels (e.g., 968 genes in [48]) upon loss of PRG-1. Another set of genes that could encode similar sensors are those identified using repeated RNAi as modifiers of transgenerational epigenetic kinetics [55]. Regardless of the identities of the sensors, differences in the transgenerational feedback that reduces some component(s) of the 22G-pUG positive feedback loop can explain the persistence of, recovery from, and resistance to heritable RNA silencing when different genes are targeted for silencing.

In summary, experimental evidence and theoretical considerations suggest that the HRDE-1-dependent positive feedback loop that generates 22G RNAs and pUG RNAs is tuned by negative feedback that acts across generations to cause different durations of heritable RNA silencing. Such tuning can explain silencing for a few generations followed by recovery from silencing as well as resistance to silencing. Future studies are required for testing the quantitative predictions on the impact of reducing 22G RNA or pUG RNA levels (Eq. (4) and (5)) and for identifying the PRG-1-dependent genes predicted to have roles in the transgenerational inhibition of heritable RNA silencing (Fig. 6D).

DISCUSSION

The framework presented here establishes criteria for (1) heritable information in regulatory architectures, (2) the persistence of epigenetic changes across generations, (3) distinguishing between regulatory architectures using transient perturbations, (4) making unstable regulatory architectures in the germline heritable through interactions with somatic cells, and (5) generating epigenetic changes of defined magnitude and duration.

ESP systems can be used to analyze many types of regulatory interactions

The simple ESP systems simulated here (Fig. 4) can be extended to include a wide variety of properties to explore heritable epigenetic changes that can occur in cell/organelle geometry, phase separation, protein folding, etc. In general, each kind of molecule or entity can have multiple properties that are sensed by different sensors. For example, concentration, folded structure, primary sequence, and subcellular localization of a protein could each be measured by different sensors that respond by causing different downstream effects. If a protein (x) is regulated by three different regulators that each change its concentration (C), subcellular localization (L), or folded structure (F), then the protein x could be considered as having C, L, and F as values for its regulated properties. If the protein x in turn acts as a regulator that changes another entity y, then the activity of x regulating y could be simulated as a combined function of its concentration, localization and folded structure (i.e., activity of $x = f(C, L, F)$). Such simulations preserve both the independent regulation of different properties of a protein along with the potential equivalence in the activity of a higher concentration of partially folded proteins and a lower concentration of well-folded proteins. Thus, appropriate mapping onto an ESP system would enable the explanation of many phenomena in terms of regulatory architectures formed by any set of interactors while rigorously considering heritability.

A positive feedback loop can only support the inheritance of one property of an entity

While no entity can promote changes in all its properties by itself, some entities can promote changes in one of their properties through self-regulatory interactions under some conditions. For example, prions can act as replicating stores of information that template changes in the conformation of other proteins with the same sequence [56], although other properties of prions such as their concentration, subcellular localization, rate of turnover, etc. are determined through interactions with other entities/sensors. Such self-regulatory interactions for the control of some properties can be considered by allowing self-referential loops. Specifically, if the protein x above were a prion, then its properties will include C, L, and F as above, with the value of F changing with time as a function of both concentration and prior proportion folded (i.e., $F(t+1) = g(C, F(t))$). Similar considerations underscore that any one positive feedback loop can promote only one property of an entity and not all of its properties. For example, consider small RNAs that are associated with gene silencing in *C. elegans*. The targeting of a gene by small RNAs could be preserved in every generation through a regulatory loop whereby recognition of

mRNA by antisense small RNAs results in the production of additional small RNAs by RNA-dependent RNA Polymerases. However, the mere existence of this feedback loop cannot explain the different concentrations of small RNAs targeting different genes [50] or the different durations of persistent small RNA production when initiated experimentally [42]. Similar considerations apply for chromatin modifications, DNA modifications, RNA modifications, and all other 'epigenetic marks'.

Mutability of epigenetic information changes non-monotonically with complexity

Inducing heritable changes in epigenetic information is more challenging than inducing similar changes in genetic information [2]. Chemically altering a single molecule (typically DNA) is sufficient for inducing a genetic change, however, similarly altering one entity of a regulatory architecture (say, a protein) to induce an epigenetic change requires simultaneously altering the many copies of that entity without altering DNA sequence. All DNA bases with induced chemical changes are deleted or converted into one of the other bases by the replication and repair pathways. As a consequence, only 6 different base exchanges are possible in DNA sequence through a single mutation, but even when only up to three interactors are considered, 61 different HRA changes are possible through a single mutation (Fig. 3). Importantly, after a heritable change, the DNA sequence remains similarly mutable, but the impact of a change (genetic or epigenetic) on subsequent mutability of a regulatory architecture could increase or decrease. Consider a change that incorporates a new transcription factor into a regulatory architecture. If it is an activator, it could promote the expression of many genes leading to the incorporation of more RNAs and proteins into the regulatory architecture. Conversely, if it is a repressor, it could repress the expression of many genes leading to the removal of RNAs and proteins from the regulatory architecture. Either of these consequences could make the entire architecture more robust such that drastic perturbation is needed to cause observable change. When such robust architectures occur during development, the identity of a cell could become relatively fixed and heritable through cell divisions and yet remain compatible with specific natural [57] and/or induced [58] cell fate transformations. Thus, such cell fate determination reflects the acquisition of different robust states, providing the appearance of a cell 'rolling down an epigenetic landscape' [59].

Complexity of heritable regulatory architectures

Despite imposing heritability, regulated non-isomorphic directed graphs soon become much more numerous than unregulated non-isomorphic directed graphs as the number of interactors increase (125 vs. 5604 for 4 interactors, Table 1). With just 10 interactors, there are $>3x10^{20}$ unregulated non-isomorphic directed graphs [60] and HRAs are expected to be more numerous. This tremendous variety highlights the vast amount of information that a complex regulatory architecture can represent and the large number of changes that are possible despite sparsity of the change matrix (Fig. 3). This number is potentially a measure of epigenetic evolvability – the ability to adapt and survive through regulatory change without genetic mutations. However, architectures made up of numerous interactors that are all necessary for the positive feedback loop(s) required for transmitting information across generations are more vulnerable to collapse (e.g., 'C' and 'T' in Fig. 1). Furthermore, spatial constraints of the bottleneck stage (one cell in most cases) presents a challenge for the robust transmission of regulatory information. A speculative possibility is that complex architectures are compressed into multiple smaller positive feedback loops for transmission between generations with the larger HRAs being re-established through interactions between the positive feedback loops in every generation. Examples of such numerous but small positive feedback loops include small RNA-mediated, chromatin-mediated, and prion-mediated loops that specify the identity of genes for particular forms of regulation in the next generation. However, determining how the rest of the regulatory information is transmitted in each case and whether such compression with redundancy is a general principle of heredity require further study.

Information Density in Living Systems

Individual entities transmitted across generations can be considered as carrying part of the heritable information if such information is always seen in the context of the sensors that interact with the entity. While the maximal information that can be carried by DNA sequence is a product of its

length (l) and the number of bits contributed by each base ($2l$ = $\log_2[4].l$), the maximal number of relevant bits contributed by any entity - including the genome - depends on the number of states sensed by all interacting sensors (for i^{th} entity = $\log_2(\sum_{j=1}^{s_i} s_j \left(\sum_{k=1}^{p_j} p_k\right))$ from equation (1)) [3]. The genome likely interacts with the largest number of sensors per molecule, making it the entity with the most information density. When a gene sequence is transcribed and translated, sequence information is transmitted from one molecule (DNA) to many (RNA(s) and/or protein(s)), thereby reducing the density of sequence information per entity (e.g., RNA or protein of a particular sequence). However, information is also added to these entities through the process of RNA folding and protein folding, which depend on interactions with the surrounding chemical and physical context (e.g., [61]). The resultant structural (and potentially catalytic) specialization of RNAs and proteins provides them with additional properties that are relevant for other sensors, thereby increasing their information content beyond that in the corresponding genome sequence. Importantly, these proteins and RNAs can interact to create molecular complexes and organelles that again concentrate information in higher-order entities present as fewer copies within cells (e.g., centrosomes). Such complexes and organelles therefore are entities with high information density. In this view, the information density throughout a bottleneck stage connecting two generations (e.g., the single-cell zygote) is non-uniform and ranges from entities with very high density (e.g., the genome) to those with very low density (e.g., water). Beginning with the simplest of regulatory architectures (Fig. 1), progressive acquisition of entities and their interacting sensors would lead to the incorporation of regulators with increasing information density. An entity that is connected to a large number of sensors that each respond to changes in a fraction of its properties can appear to be the chief 'information carrier' of the living system (e.g., DNA in cells with a genome). Thus, as heritable regulatory architectures evolve and become more complex, entities with a large number of sensed properties can appear central or controlling (see [62, 63] for similar ideas). This pathway for increasing complexity through interactions since before the origin of life outlines how any form of high-density information storage can be used to construct what appears to be the key information carrier in a living system – a new kind of DNA for a new kind of life.

METHODS SUMMARY

Software. All calculations were performed by hand or using custom programs in Python (v. 3.8.5), and/or R (v. 3.6.3). Simulations and analyses were performed using NetLogo (v. 6.1.1), Python (v. 3.8.5), and/or R (v. 3.6.3). Transitions between HRAs were depicted using the circular layout plugin in Gephi (v. 0.10.1 202301172018).

Analysis of heritable regulatory architectures. The possible weakly connected non-isomorphic graphs that form regulatory architectures capable of indefinite persistence and the maximal information that can be stored using them ($\log_2$N) were calculated. Systems of ordinary differential equations (ODEs) were used to describe the rate of change for each interacting entity (x, y, z) in each of the 26 heritable regulatory architectures (A to Z) with the relative amounts of all entities at any time defined as the 'phenotype' at that time. Each regulatory architecture is characterized by a maximum of 9 parameters in addition to the relative amounts of each entity: a rate of turnover for each entity (3 total; T_x, T_y, T_z) and rates for each regulatory interaction between entities (6 total; e.g., k_{xy} is the regulatory input to x from y, k_{yz} is the regulatory input to y from z, etc.). Relative amounts of each interacting entity for each architecture at steady state (x_0, y_0, z_0) were determined by setting all rate equations to zero, which results in constraints on the variables for each architecture (e.g., for A: $y_0 = x_0.\frac{T_x}{k_{xy}} = x_0.\frac{k_{yx}}{T_y}$; for B: $y_0 = x_0.\frac{T_x}{k_{xy}} = x_0.\frac{k_{yx}}{T_y}$; $z_0 = x_0.\frac{T_x}{k_{xy}}.\frac{k_{zy}}{T_z}$, etc. See supplemental methods for the steady-state constraints for all architectures). These constraints were used to obtain a total of 128,015 parameter sets ($T_x, T_y, T_z, k_{xy}, k_{yz}$, etc.) that are compatible with steady state for each architecture (Table S1). Particular parameter sets were then used to illustrate the consequences of genetic and epigenetic changes in all architectures (Fig. 2 and Figs. S3 – S9). The simpler expressions for steady-state levels for all regulatory architectures when there are no turnover mechanisms for any entities and the only 'turnover' occurs by dilution upon cell division ($T = T_x =$

$T_y = T_z$) were derived (see supplementary information). Expressions for steady state values when all entities are lost at a constant rate to complex formation (γ) and for changes upon complete loss of an entity were also derived (see supplementary information).

The impacts of transient perturbations from steady state were examined for each architecture to identify conditions for heritable epigenetic change by defining thresholds (d_x, d_y, d_z) for observing a defect for each entity (e.g., for the function of x, $d_x.x_0$ is not sufficient, when $d_x < 1$, or $d_x.x_0$ is in excess, when $d_x > 1$). Responses after perturbations are illustrated for all architectures (Figs. S3 to S9) and cases where genetic and epigenetic perturbations result in distinct responses are highlighted (Fig. 2). The duration and extent of perturbation needed for heritable epigenetic changes were explored using numerical solutions of the equations describing the dynamics of each regulatory architecture. Explorations of 22G-pUG positive feedback loop were similarly performed by simulating a type 'A' HRA using ODEs (Fig. 6). Analytical expressions for conditions that enable heritable epigenetic change were derived for the simplest heritable regulatory architecture where two entities (x and y) mutually promote each other's production. Transitions between HRAs (Fig. 3) were worked out manually by considering the consequence of each change from steady state for each HRA.

Analysis of entity-sensor-property systems. Simple ESP systems were simulated using custom programs in NetLogo [26](details are available within the 'code' and 'info' tabs of each program). Results from systematic explorations obtained by running NetLogo programs from the command line (i.e., 'headless') were analyzed using R (e.g., Fig. 4D, Fig. S12). The developmental timing of cell division is *C. elegans* were curated manually from the literature (Table S3) and used to simulate ESP systems that incorporate this developmental timing and temporal delays in regulation (Fig. 5). Supplementary movies (Movie S1 – S13) were made by recording screen captures of NetLogo runs using QuickTime Player.

Data availability

All programs used in this study (written in NetLogo (v. 6.1.1), Python (v. 3.8.5), and/or R (v. 3.6.3)) are available at https://github.com/AntonyJose-Lab/Jose_2023.

ACKNOWLEDGEMENTS

The author thanks Thomas Kocher, Pierre-Emanuel Jabin, Todd Cooke, Charles Delwiche, and Karen Carleton for discussions; and Thomas Kocher, Pierre-Emanuel Jabin, and members of the Jose Lab for comments on the manuscript. This work was supported in part by National Institutes of Health Grant R01GM124356, National Science Foundation Grant 2120895, and FRSA from UMD to A.M.J. The Author declares no competing interests.

TABLES, FIGURES, AND FIGURE LEGENDS

Entities	Heritable	Regulated	Heritably regulated	Bits of information
1	0	0	0	-
2	1	3	1	0
3	7	96	25	4.64
4	125	19559	5604	12.45

Table 1. Capacity of heritable regulatory architectures to store information. The number of heritable, regulated, and heritably regulated architectures, and the information they can store were calculated using a program that enumerates non-isomorphic weakly connected graphs that satisfy specified criteria (‘Heritable_Regulatory_Architectures_1-4_entities.py’).

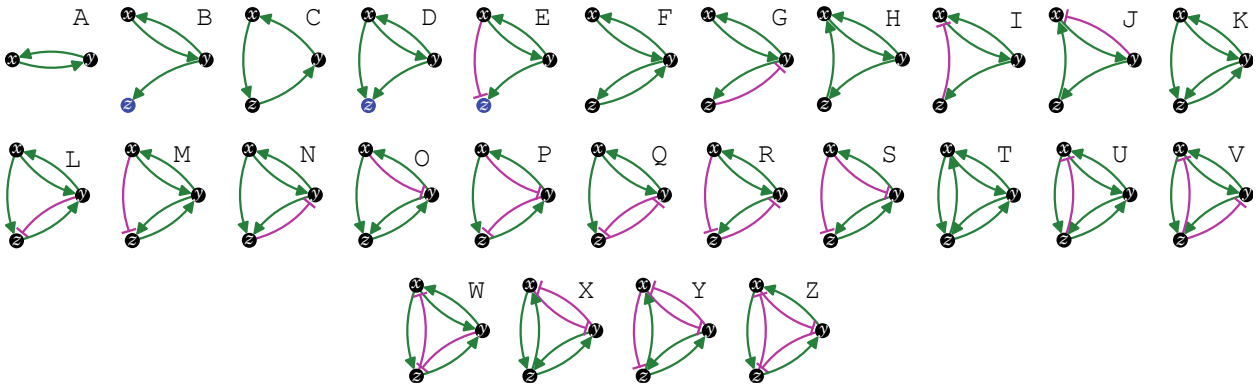

Figure 1. The simplest heritable regulatory architectures. Of the 99 possible regulatory architectures with fewer than four entities (see Fig. S2), only 26 can be indefinitely heritable (A through Z with *x*, *y*, and *z* entities/sensors). Entities that act as sensors (black circles) or that do not provide any regulatory input (blue circles), positive (green arrows) and negative (magenta bar) regulatory interactions are indicated.

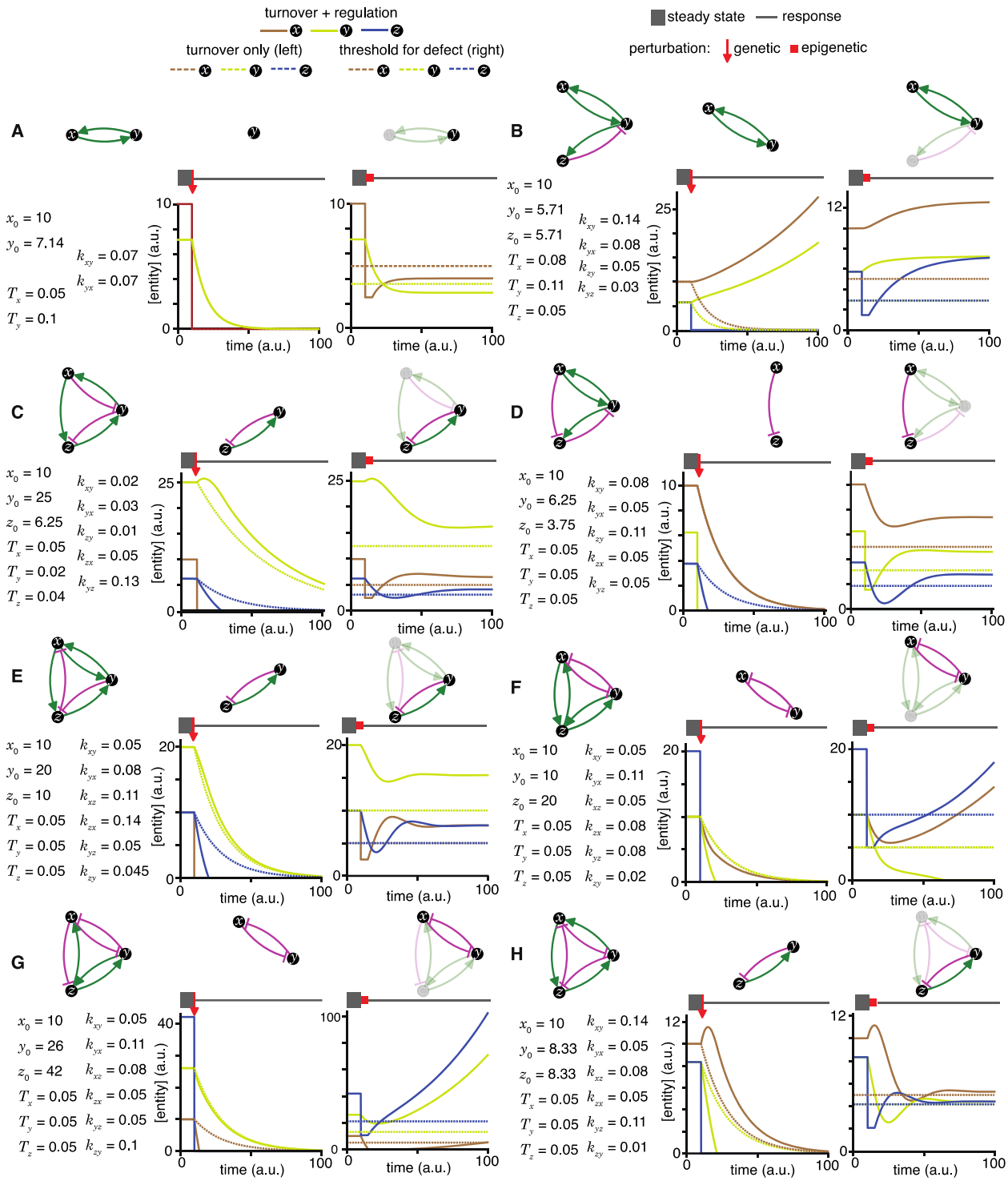

Figure 2. Epigenetic and genetic changes can provide complementary information about heritable regulatory architectures. (A to H) In each panel, cases where specific perturbations of architectures (*top left*) characterized by sets of parameters that support a steady state (*bottom left*) result in different outcomes for permanent or genetic (*middle*) versus transient or epigenetic (*right*) changes are illustrated. Relative concentrations of each entity during periods of steady state (thick grey line), the point of genetic change (red arrow), periods of epigenetic reduction (red bar, for a duration t_p = 5 (a.u); with the threshold for observing a defect d = 0.5; and an extent of perturbation beyond the threshold p = 0.5), and periods of

recovery after perturbation (thin grey line) are shown. Architectures are depicted as in Figure 1 (A, B, C, D, E, F, G, and H depict the heritable regulatory architectures A, G, P, R, W, X, Y and Z, respectively) with transient reductions in an entity or sensor and associated interactions depicted using lighter shades. Dotted lines indicate unregulated turnover (in *middle*) or thresholds for observing defects upon reduction in levels of an entity/sensor (in *right*).

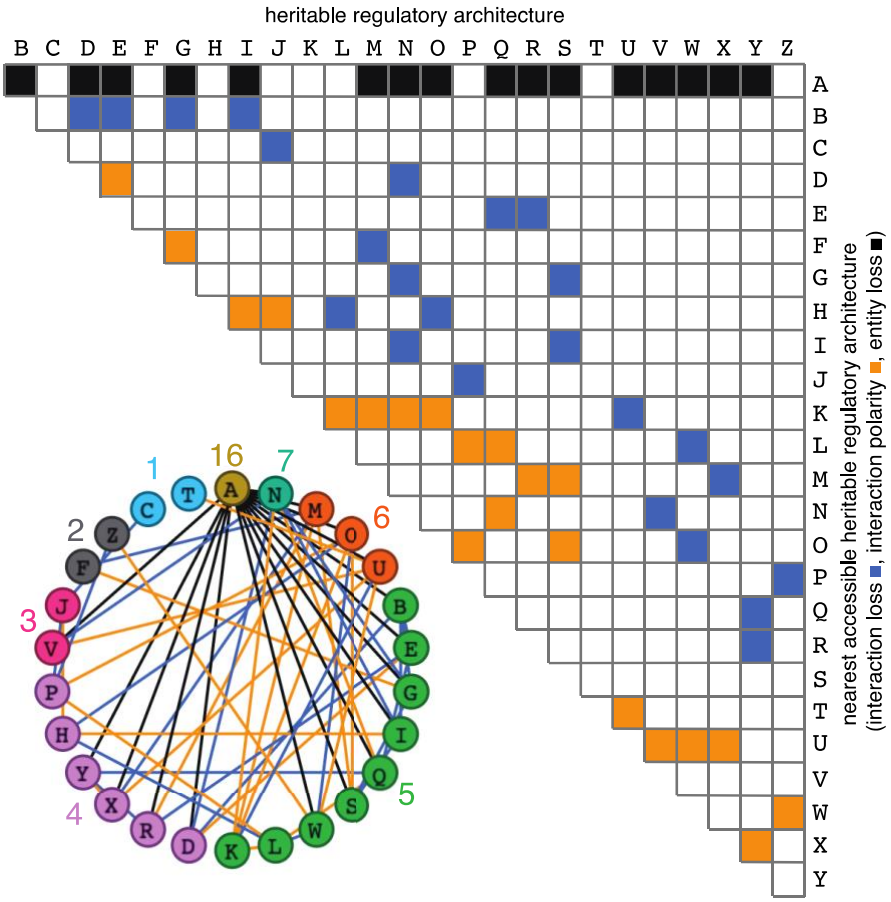

Figure 3. Possible conversions between the simplest heritable regulatory architectures. Table summarizing the possible changes in regulatory architecture observed after a single perturbation from steady state (blue, loss of a regulatory interaction; orange, change in the polarity of a regulatory interaction; black, either change in regulatory interaction and/or loss of an entity). For example, Z can arise from P through the loss of a regulatory interaction or from W through a change in the polarity of a regulatory interaction. *Bottom left*, Network diagram summarizing possible changes arranged clockwise by frequency of change to the HRA (color-matched numbers). Edges (black, blue, or orange) are colored as in table and nodes are colored according to number of adjacent HRAs.

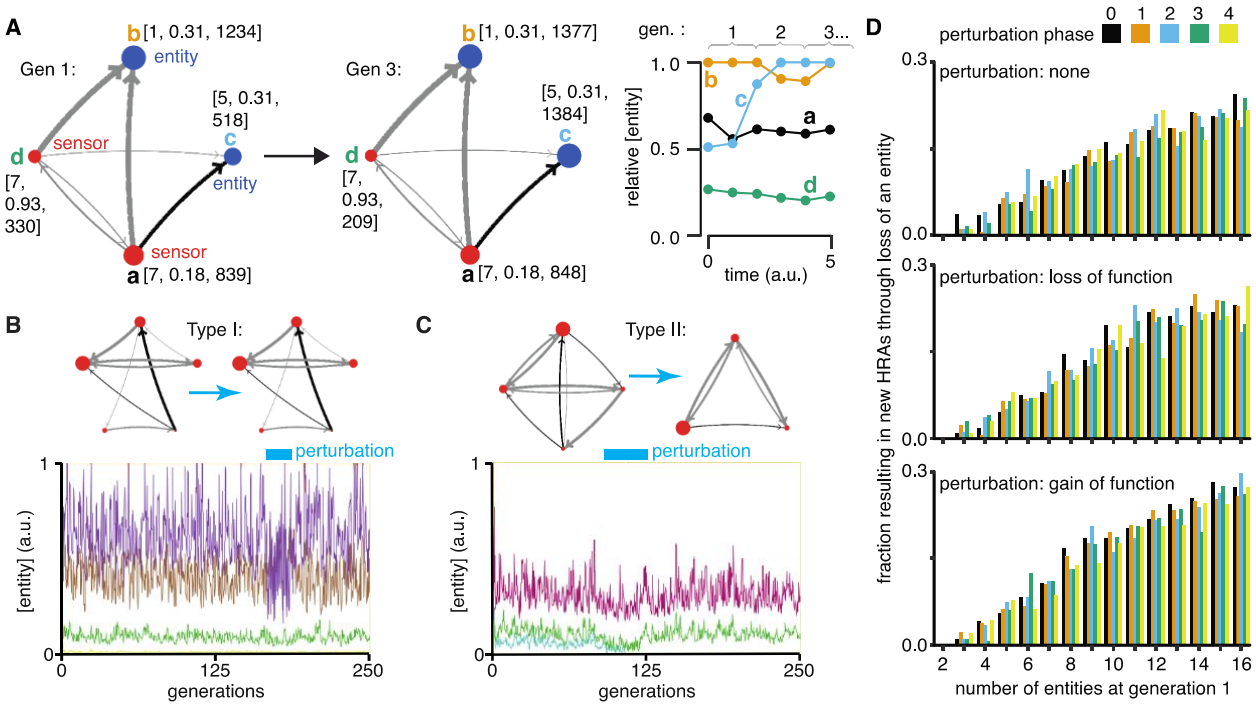

Figure 4. Regulatory architectures can be simulated as entity-sensor-property systems to examine how they persist or change in response to transient perturbations. (A) An ESP system illustrating the stability of a regulatory architecture despite changes in the relative numbers of the interactors (entities/sensors) over time. *Left*, Simulation of an ESP system showing how interacting molecules create regulatory architectures. This system consists of four entities (a, b, c, d), where 'd' and 'a' are also sensors. Each sensor (red) sends regulatory input (grey, positive or black, negative) to increase or decrease another sensor or entity (blue). Numbers of each entity (i.e., its property value) change in fixed steps per unit time. The number of sensors needed to cause one unit of change in property differs for each regulatory input (lower number = thicker line, representing lower threshold for downstream change). Each entity is depicted with property step, active fraction, and number at the start of the first generation (gen 1) and at the end of the third generation (gen 3). *Right*, The relative numbers of the entities, which can be together considered as 'phenotype', can change over time. Note that relative amounts of 'a', 'b', or 'd' remain fairly constant, but that of 'c' changes over time. (B and C) ESP systems can differ in their response to epigenetic change. *Top*, ESP systems are depicted as in A. *Bottom*, Relative abundance of each entity/sensor (different colors) or 'phenotype' across generations. Blue bars = times of epigenetic perturbation (reduction by two fold). In response to epigenetic perturbation that lasts for a few generations, Type I systems recover without complete loss of any entity/sensor (B) and Type II systems change through loss of an entity/sensor (C). (D) ESP systems of varying complexity can show heritable epigenetic changes, depending on when the system is perturbed. The numbers of randomly chosen entities were unperturbed (none, *top*), reduced to half the minimum (loss of function), or increased to twice the maximum (gain of function, *bottom*) every 50 generations for 2.5 generations and the number of systems responding with a new stable regulatory architecture that lasts for >25 generations were determined. Perturbations were introduced at each of five different time points with respect to the starting generation (phase - 0,1,2,3,4). Of the 78,285 stable systems, 14,180 showed heritable epigenetic change.

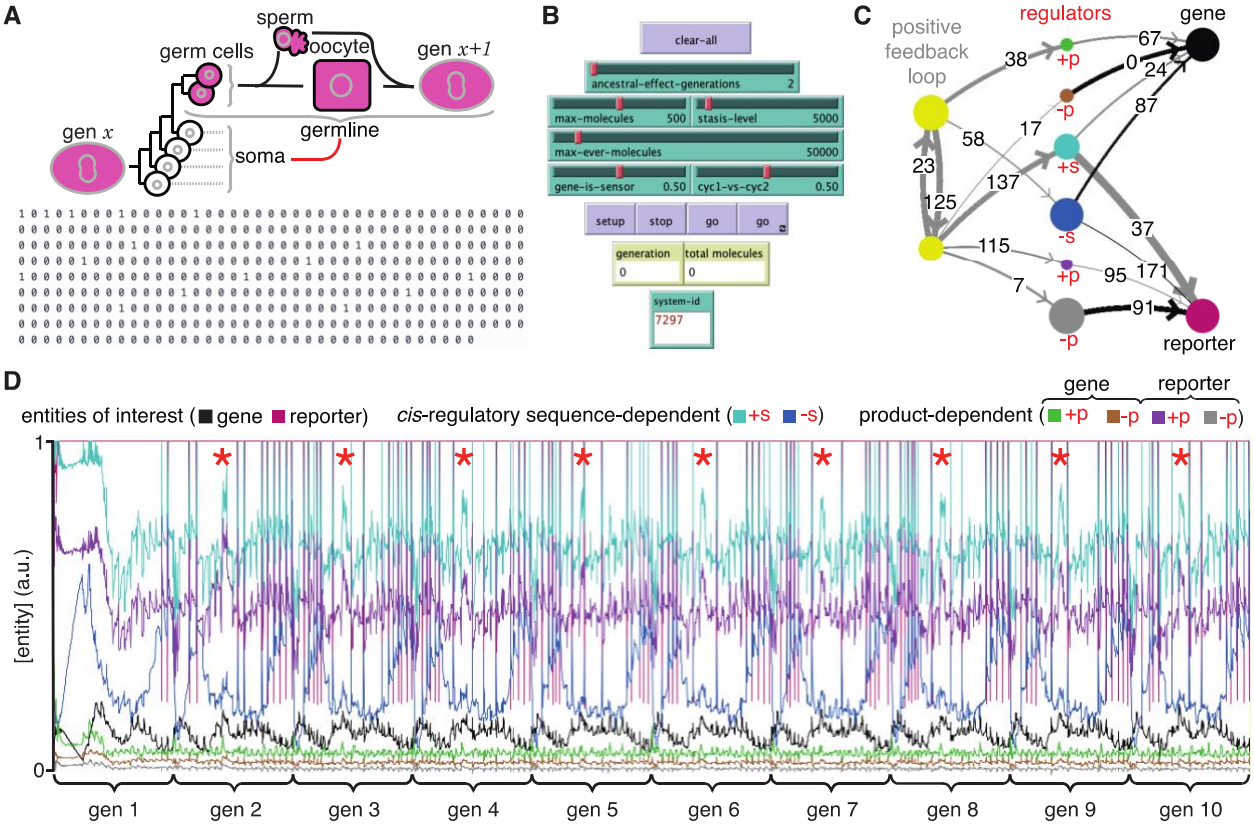

Figure 5. ESP systems that incorporate the timings of cell division during *C. elegans* development and temporal delays in regulatory interactions can recreate periods of increased expression in every generation. (A) *Top*, Schematic of cell divisions between two successive generations of *C. elegans*. Cells that maintain the intergenerational continuity through cell divisions (magenta, germline), cells that cannot contribute to the next generation through cell divisions (white, soma) but arise in each generation (gen *x* and gen *x+1*) from the bottleneck stage, and the interactions between these two cell types (red line) are depicted. *Bottom*, Experimentally determined timing of cell division (1) versus growth (0) from one zygote to the next in *C. elegans* in 15 minute intervals (= 1 time step in simulations), which give a generation time of ~91.25 hours (= 365 time steps). See Table S3 for the relative timing of cell divisions based on past studies. (B) Key control features for simulating HRAs that incorporate organismal timing of cell divisions and temporal delays in regulation. In addition to controls used in the single system explorer (Fig. S10A), the following sliders were added: one to set the number of generations of ancestors that can contribute regulation (ancestral-effect-generations, e.g., 2 for parental effects), one to set the probability of the regulatory origin for each interaction from one of the two sensors that form the positive feedback loop required for heritability (cyc1-vs-cyc2), and one to set the probability of the gene of interest being a sensor providing regulatory input into the positive feedback loop instead of an entity (gene-is-sensor). Monitors that show the current generation and the total number of molecules, and an input to set the system-id were also added. (C) Representative simulated HRA that incorporates temporal delays and the characteristic timings of cell divisions in *C. elegans*. Different types of positive (+) and negative (-) regulators (red) that depend on *cis*-regulatory sequences (+s and -s, e.g., transcription factors), and that depend on the gene product (+p and -p for gene and reporter, e.g., small RNAs made using mRNA template, chaperones that promote the folding of the protein, etc.) are depicted with color coded arrows (+, grey and -, black). Different relative delays in regulation (hours on arrows, maximum of 2x generation time to allow for the widely observed parental regulation) are also depicted. The unknown components of the core positive feedback loops required for heredity were simulated as two sensors that promote each other's production

in addition to the production of all other entities/sensors. (D) Relative concentrations of entities/sensors regulated by the HRA in (C) over 10 generations showing transgenerational waveforms. Properties, active fractions, relative numbers, and regulatory interactions were considered and relative numbers of each entity/sensor depicted as in Fig. 4 with colors as in (C). Although the simulation began with random numbers for all entities/sensors, the HRA settles into a reproducible pattern within two generations with periods of increased relative concentrations for some entities/sensors in every generation (red asterisks). Also see Movie S13.

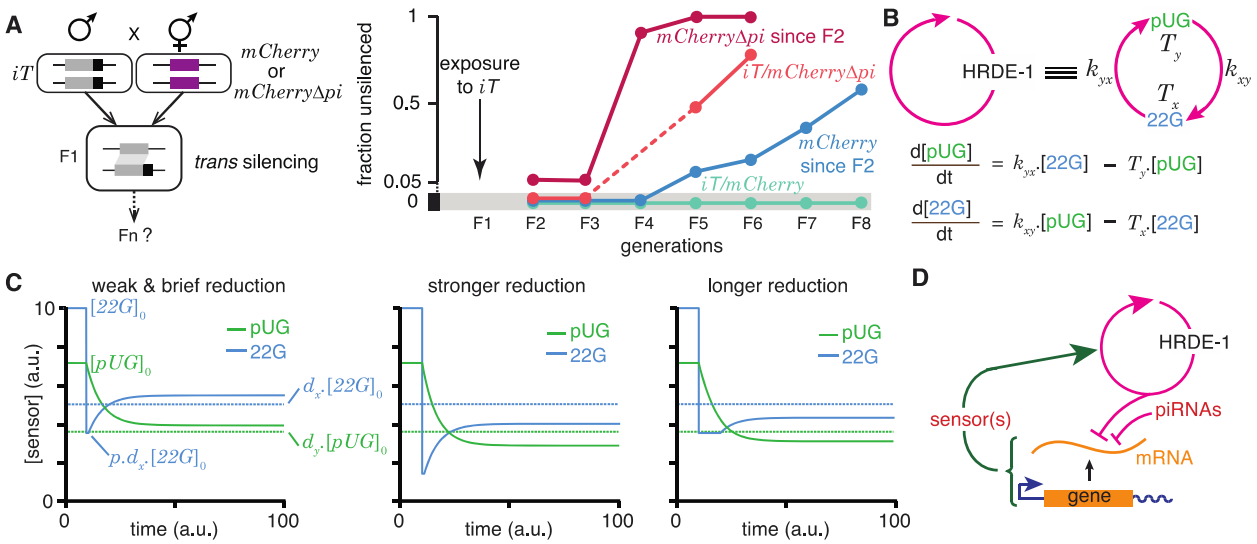

Figure 6. Regulation of a positive feedback loop can explain the magnitude and duration of experimentally observed heritable RNA silencing. (A) Experimental evidence from *C. elegans* for susceptibility to, recovery from, and resistance to *trans* silencing by a silenced gene (adapted from [42]). *Left*, Schematic of experiment showing a gene silenced for hundreds of generations by mating-induced silencing (*iT = mex-5p::mCherry::h2b::tbb-2 3' utr::gpd-2 operon::gfp::h2b::cye-1 3' utr*) exposed to genes with matching sequences (*mCherry* and *mCherryΔpi*, i.e., *mCherry* without piRNA binding sites) to initiate *trans* silencing. *Right*, Dynamics of heritable RNA silencing showing the initial exposure to *trans* silencing by *iT* (F1 generation), subsequent recovery after separation from *iT* ('*mCherry* since F2' and '*mCherryΔpi* since F2'), resistance to silencing by *iT* (*iT/mCherryΔpi*), or persistence of silencing by *iT* (*iT/mCherry*). Fractions of animals that recover *mCherry* or *mCherryΔpi* expression (fraction unsilenced) are depicted with error bars eliminated for simplicity. (B) Abstraction of the HRDE-1-dependent positive feedback loop required for the persistence of RNA silencing. *Top*, Representation of the mutual production of RNA intermediates (22G and pUG) with rates of production (k_{yx} and k_{xy}) and turnover (Tx and T_y). *Bottom*, Ordinary differential equations for the rates of change of pUG RNAs (pUG) and 22G RNAs (22G). See text for details. (C) Impact of transient epigenetic perturbations on subsequent activity of a positive feedback loop. *Left*, response to a brief and weak reduction in the levels of one sensor (22G) of the positive feedback loop. The steady-state levels after recovery were above the threshold required for a silencing effect (dotted lines). Steady states ($[22G]_0$ and $[pUG]_0$), perturbation level ($p.d_x.[22G]_0$), and levels required for silencing ($d_x.[22G]_0$ and $d_y.[pUG]_0$) are indicated. *Middle* and *Right*, Stronger (*middle*) or longer (*right*) reduction can result in steady-state levels after recovery being below the threshold required for a silencing effect (dotted lines). (D) Deduced regulatory architecture that explains data shown in (A) by including enhancement of silencing by piRNA binding on target mRNA and a gene-specific inhibitory loop that can act across generations through as yet unidentified sensor(s). Prolonged silencing in *prg-1(-)* animals [43] suggests that these sensor(s) are among the genes mis-regulated in *prg-1(-)* animals (e.g., [48]). See Fig. S13 for depictions of additional equivalent architectures.

References

1. A. M. Jose, Replicating and Cycling Stores of Information Perpetuate Life. *Bioessays* **40**, e1700161 (2018).
2. A. M. Jose, Heritable Epigenetic Changes Alter Transgenerational Waveforms Maintained by Cycling Stores of Information. *Bioessays* **42**, e1900254 (2020).
3. A. M. Jose, A framework for parsing heritable information. *J R Soc Interface* **17**, 20200154 (2020).
4. A. M. Jose, The analysis of living systems can generate both knowledge and illusions. *Elife* **9** (2020).
5. S. Alberti, A. Gladfelter, T. Mittag, Considerations and Challenges in Studying Liquid-Liquid Phase Separation and Biomolecular Condensates. *Cell* **176**, 419-434 (2019).
6. D. Krakauer, N. Bertschinger, E. Olbrich, J. C. Flack, N. Ay, The information theory of individuality. *Theory Biosci* **139**, 209-223 (2020).
7. M. Eigen, Selforganization of matter and the evolution of biological macromolecules. *Naturwissenschaften* **58**, 465-523 (1971).
8. T. Ganti, Organization of chemical reactions into dividing and metabolizing units: the chemotons. *Biosystems* **7**, 15-20 (1975).
9. F. G. Varela, H. R. Maturana, R. Uribe, Autopoiesis: The organization of living systems, its characterization and a model. *Biosystems* **5**, 187-196 (1974).
10. S. A. Kauffman, *The origins of order* (Oxford University Press, 200 Madison Avenue, New York, New York, 10016, 1993), pp. 709.
11. A. Y. Mitrophanov, E. A. Groisman, Positive feedback in cellular control systems. *Bioessays* **30**, 542-555 (2008).
12. U. Alon, *An Introduction to Systems Biology*, Chapman & Hall/CRC Computational Biology Series (CRC Press, Taylor & Francis Group, ed. 2nd, 2020), pp. 324.
13. A. V. Anzalone, L. W. Koblan, D. R. Liu, Genome editing with CRISPR-Cas nucleases, base editors, transposases and prime editors. *Nat Biotechnol* **38**, 824-844 (2020).
14. A. Fire, S. Xu, M. K. Montgomery, S. A. Kostas, S. E. Driver, C. C. Mello, Potent and specific genetic interference by double-stranded RNA in Caenorhabditis elegans. *Nature* **391**, 806-811 (1998).
15. M. Chey, A. M. Jose, Heritable epigenetic changes at single genes: challenges and opportunities in Caenorhabditis elegans. *Trends Genet* **38**, 116-119 (2022).
16. L. Robert, G. Paul, Y. Chen, F. Taddei, D. Baigl, A. B. Lindner, Pre-dispositions and epigenetic inheritance in the Escherichia coli lactose operon bistable switch. *Mol Syst Biol* **6**, 357 (2010).
17. M. Merdanovic *et al.*, Activation by substoichiometric inhibition. *Proc Natl Acad Sci U S A* **117**, 1414-1418 (2020).
18. A. L. Barabasi, Z. N. Oltvai, Network biology: understanding the cell's functional organization. *Nat Rev Genet* **5**, 101-113 (2004).
19. M. Levine, E. H. Davidson, Gene regulatory networks for development. *Proc Natl Acad Sci U S A* **102**, 4936-4942 (2005).
20. T. Li *et al.*, A scored human protein-protein interaction network to catalyze genomic interpretation. *Nat Methods* **14**, 61-64 (2017).
21. M. Costanzo *et al.*, Global Genetic Networks and the Genotype-to-Phenotype Relationship. *Cell* **177**, 85-100 (2019).
22. E. U. Azeloglu, R. Iyengar, Signaling networks: information flow, computation, and decision making. *Cold Spring Harb Perspect Biol* **7**, a005934 (2015).
23. Y. Wan *et al.*, Dynamic imaging of nascent RNA reveals general principles of transcription dynamics and stochastic splice site selection. *Cell* **184**, 2878-2895 e2820 (2021).
24. K. Van den Berge *et al.*, RNA Sequencing Data: Hitchhiker's Guide to Expression Analysis. *Annual Review of Biomedical Data Science* **2**, 139-173 (2019).
25. A. Mund, A. D. Brunner, M. Mann, Unbiased spatial proteomics with single-cell resolution in tissues. *Mol Cell* **82**, 2335-2349 (2022).
26. U. Wilensky (1999) NetLogo. in *Center for Connected Learning and Computer-Based Modeling, Northwestern University, Evanston, IL*.
27. A. K. Corsi, A biochemist's guide to Caenorhabditis elegans. *Anal Biochem* **359**, 1-17 (2006).
28. J. Marre, E. C. Traver, A. M. Jose, Extracellular RNA is transported from one generation to the next in Caenorhabditis elegans. *Proc Natl Acad Sci U S A* **113**, 12496-12501 (2016).
29. A. E. Dodson, S. Kennedy, Germ Granules Coordinate RNA-Based Epigenetic Inheritance Pathways. *Dev Cell* **50**, 704-715 e704 (2019).
30. I. Lev *et al.*, Germ Granules Govern Small RNA Inheritance. *Current Biology* **29**, 2880-2891 e2884 (2019).
31. J. P. T. Ouyang *et al.*, P Granules Protect RNA Interference Genes from Silencing by piRNAs. *Dev Cell* **50**, 716-728 e716 (2019).

32. Y. Abdu, C. Maniscalco, J. M. Heddleston, T. L. Chew, J. Nance, Developmentally programmed germ cell remodelling by endodermal cell cannibalism. *Nat Cell Biol* **18**, 1302-1310 (2016).
33. K. Oegema, A. A. Hyman, Cell division. *WormBook* 10.1895/wormbook.1.72.1, 1-40 (2006).
34. Z. Bao, Z. Zhao, T. J. Boyle, J. I. Murray, R. H. Waterston, Control of cell cycle timing during C. elegans embryogenesis. *Dev Biol* **318**, 65-72 (2008).
35. C. A. Giurumescu *et al.*, Quantitative semi-automated analysis of morphogenesis with single-cell resolution in complex embryos. *Development* **139**, 4271-4279 (2012).
36. J. Kimble, S. L. Crittenden, Germline proliferation and its control. *WormBook* 10.1895/wormbook.1.13.1, 1-14 (2005).
37. A. Jaramillo-Lambert, M. Ellefson, A. M. Villeneuve, J. Engebrecht, Differential timing of S phases, X chromosome replication, and meiotic prophase in the C. elegans germ line. *Dev Biol* **308**, 206-221 (2007).
38. D. Hirsh, D. Oppenheim, M. Klass, Development of the reproductive system of Caenorhabditis elegans. *Dev Biol* **49**, 200-219 (1976).
39. M. H. Fitz-James, G. Cavalli, Molecular mechanisms of transgenerational epigenetic inheritance. *Nat Rev Genet* **23**, 325-341 (2022).
40. S. Catania *et al.*, Evolutionary Persistence of DNA Methylation for Millions of Years after Ancient Loss of a De Novo Methyltransferase. *Cell* **180**, 263-277 e220 (2020).
41. N. Frolows, A. Ashe, Small RNAs and chromatin in the multigenerational epigenetic landscape of Caenorhabditis elegans. *Philos Trans R Soc Lond B Biol Sci* **376**, 20200112 (2021).
42. S. Devanapally *et al.*, Mating can initiate stable RNA silencing that overcomes epigenetic recovery. *Nat Commun* **12**, 4239 (2021).
43. A. Shukla, R. Perales, S. Kennedy, piRNAs coordinate poly(UG) tailing to prevent aberrant and perpetual gene silencing. *Curr Biol* **31**, 1-13 (2021).
44. M. Priyadarshini, J. Z. Ni, A. M. Vargas-Velazquez, S. G. Gu, C. Frokjaer-Jensen, Reprogramming the piRNA pathway for multiplexed and transgenerational gene silencing in C. elegans. *Nat Methods* **19**, 187-194 (2022).
45. B. A. Buckley *et al.*, A nuclear Argonaute promotes multigenerational epigenetic inheritance and germline immortality. *Nature* **489**, 447-451 (2012).
46. A. Shukla *et al.*, poly(UG)-tailed RNAs in genome protection and epigenetic inheritance. *Nature* **582**, 283-288 (2020).
47. M. Seth *et al.*, The Coding Regions of Germline mRNAs Confer Sensitivity to Argonaute Regulation in C. elegans. *Cell Rep* **22**, 2254-2264 (2018).
48. K. J. Reed *et al.*, Widespread roles for piRNAs and WAGO-class siRNAs in shaping the germline transcriptome of Caenorhabditis elegans. *Nucleic Acids Res* **48**, 1811-1827 (2020).
49. O. Karin, E. A. Miska, B. D. Simons, Epigenetic inheritance of gene silencing is maintained by a self-tuning mechanism based on resource competition. *Cell systems* **14**, 24-40.e11 (2023).
50. W. Gu *et al.*, Distinct argonaute-mediated 22G-RNA pathways direct genome surveillance in the C. elegans germline. *Mol Cell* **36**, 231-244 (2009).
51. J. Pak, J. M. Maniar, C. C. Mello, A. Fire, Protection from feed-forward amplification in an amplified RNAi mechanism. *Cell* **151**, 885-899 (2012).
52. M. Shirayama *et al.*, piRNAs initiate an epigenetic memory of nonself RNA in the C. elegans germline. *Cell* **150**, 65-77 (2012).
53. D. R. Knudsen, P. Raman, F. Ettefa, L. De Ravin, A. M. Jose, Target-specific requirements for RNA interference can be explained by a single regulatory network. *bioRxiv* 10.1101/2023.02.07.527351v1 (2023).
54. R. Perales, D. Pagano, G. Wan, B. D. Fields, A. L. Saltzman, S. G. Kennedy, Transgenerational Epigenetic Inheritance Is Negatively Regulated by the HERI-1 Chromodomain Protein. *Genetics* **210**, 1287-1299 (2018).
55. L. Houri-Ze'evi *et al.*, A Tunable Mechanism Determines the Duration of the Transgenerational Small RNA Inheritance in C. elegans. *Cell* **165**, 88-99 (2016).
56. C. Scheckel, A. Aguzzi, Prions, prionoids and protein misfolding disorders. *Nat Rev Genet* **19**, 405-418 (2018).
57. S. Jarriault, Y. Schwab, I. Greenwald, A Caenorhabditis elegans model for epithelial-neuronal transdifferentiation. *Proc Natl Acad Sci U S A* **105**, 3790-3795 (2008).
58. Y. Shi, H. Inoue, J. C. Wu, S. Yamanaka, Induced pluripotent stem cell technology: a decade of progress. *Nat Rev Drug Discov* **16**, 115-130 (2017).

59. C. H. Waddington, *The Strategy of the Genes* (George Allen & Unwin Ltd, Museum Street, London, 1957).
60. N. J. A. Sloane, The On-Line Encyclopedia of Integer Sequences [Sloane's A003085 accessed on 1/23/2021]. https://oeis.org (2021).
61. L. L. Porter, L. L. Looger, Extant fold-switching proteins are widespread. *Proc Natl Acad Sci U S A* **115**, 5968-5973 (2018).
62. F. J. Dyson, A Model for the Origin of Life. *Journal of Molecular Evolution* **18**, 344-350 (1982).
63. D. Noble, Genes and causation. *Philos Trans A Math Phys Eng Sci* **366**, 3001-3015 (2008).